Delta University Scientific Journal
Journal home page: https://dusj.journals.ekb.eg

Removal of Methyl orange (MO) from aqueous solution by bimetal-organic frameworks (Cu_x-Cr_{100-x}–MOF): Kinetics and isotherms studies

Reda. S. Salama[1*], Sohier. A. El-Hakam[2], Salem. E. Samra[2], Shady. M. El-Dafrawy[2], Amr Awad Ibrahim[2], and Awad I. Ahmed[2]

[1] *Basic Science Department, Faculty of Engineering, Delta University for Science and Technology, Gamasa, Egypt*

[2] *Chemistry Department, Faculty of science, Mansoura University, Mansoura, Egypt*

* Corresponding author at: Basic Science Department, Faculty of Engineering, Delta University for Science and Technology, Gamasa, Egypt., Tel.: +201061391656; e-mail address: reda.salama@deltauniv.edu.eg, dr.reda.salama@gmail.com (R. S. Salama).

ABSTRACT

The kinetics studies methyl orange adsorption from aqueous solution, by using by bimetal-organic frameworks (Cux-Cr100-x–MOF), were investigated spectrophotometrically using the batch technique. Batch experiments were conducted to study the effects of pH and initial concentration of adsorbate dye adsorption. The kinetic data obtained from different batch experiments were analyzed using both pseudo first-order and pseudo second-order equations. The equilibrium adsorption data were analyzed by using the Freundlich and Langmuir models. The best results were achieved with the pseudo second-order kinetic model and with the Langmuir isotherm equilibrium model. The equilibrium adsorption capacity (qe) increases with increasing the initial concentration of dye and with decreasing pH.

Keywords: Mixed MOFs; Cu-BDC; Cr-MIL-101; methyl orange; adsorption; water treatment.

1. Introduction

Synthetic dyes are widely used for textile dyeing, paper printing, leather dyeing, color photography and as additives in petroleum products (Radha et al. 2005). They exhibit a wide range of different chemical structures, primarily based on substituted aromatic and heterocyclic groups. There are more than 100,000 dyes available commercially, most of which are difficult to biodegrade due to their centupled structure and synthetic origin (Alzaydien 2015; Puvaneswari, Muthukrishnan, and Gunasekaran 2006). The presence of very low concentrations of dyes in effluent is high visible and undesirable. Colored agents interfere with the transmission of light through water and hinder photosynthesis. Most of these dyes are harmful, when they are in contact with living tissues for a long time (Crini 2006). Physico–chemical or chemical treatment of such wastewater is however possible.

A variety of azo dyes find use in the food and textile industries. However, most of these dyes are highly carcinogenic even when present in minute quantities. Methyl orange (MO) is a carcinogenic water-soluble azo dye which is widely used in textile industries, in manufacturing printing paper, and in research laboratories. It is also metabolized into aromatic amines by intestinal microorganisms (Ma et al. 2012; Zhang and Fang 2006). Methyl orange is stable, shows low biodegradability and is soluble in water hence it is difficult to remove from aqueous solutions by common water purification/treatment methods (Suciu et al. 2012).

Many investigators have studied different techniques for removal of colored dye from wastewater such as biological treatment, adsorption, chemical oxidation, coagulation, membrane filtration and photochemical degradation (Alshorifi et al. 2021; Altass et al. 2022; Altass, Morad, et al. 2021; Bakry et al. 2022; Sohier A El-Hakam et al. 2022; El-Yazeed et al. 2022; Mannaa et al. 2021). Among them, adsorption has become the most popular technique because of its effectiveness, operational simplicity, low cost and low energy requirements (S.A. El-Hakam et al. 2018; Nigam 2007; R. S. Salama et al. 2018b). In the past few years, many waste materials or by-products have been investigated as adsorbents for removing dyes from water. The use of metal organic frameworks (MOFs) as adsorbents have received much attention because the unique structural and surface properties of these materials offer high chemical stabilities and specific surface areas that lead to high adsorption capacities (S A El-

Hakam et al. 2013; Reda S. Salama Salem. E. Samra, Shady M. El-Dafrawy and Awad I. Ahmed 2018; R. Salama et al. 2022; R. S. Salama 2019; R. S. Salama et al. 2018a).

Metal–organic frameworks (MOFs) have generated huge scientific attention as a new class of materials because of their distinctive high specific surface areas, high crystallinity, excellent porosity, diverse functionality, uniform but tunable cavities and high modularity (Eddaoudi et al. 2001) that make them display potential in a wide range of applications like catalysis (R. S. Salama et al. 2018c; Shady et al. 2019), gas storage (Li, Kuppler, and Zhou 2009), dye adsorption (Chen et al. 2012), smart sensors (Hu, Deibert, and Li 2014), separation (Li, Sculley, and Zhou 2011) and drug delivery (Horcajada et al. 2011). Their structures contain extended co-ordination networks of metal centers as nodes connected by organic ligands as linkers which offers enormous structural and chemical diversity. These exclusive properties of metal organic frameworks offer an uncountable chance to produce specific required active sites and makes MOFs excellent applicants for a variety of applications (Ranocchiari and van Bokhoven 2011).

Multivariate (MTV-MOFs) or mixed-component (MC-MOFs) metal organic frameworks represents the incorporation of several metal ions (Shady et al. 2019; Sun et al. 2015; Wang et al. 2014) or multiple organic functionalities (Sahiner, Demirci, and Yildiz 2017) within one structure resulting in materials with a higher catalytic activity. Basically, some original studies have previously revealed that the mixed-metal MOFs had superior properties over parent MOFs and in some cases, can even induce new functionalities (Altass, Khder, et al. 2021; El-Dafrawy et al. 2020; S. A. El-Hakam et al. 2021; Sohier A. El-Hakam et al. 2018; Ibrahim et al. 2021; Mannaa, Altass, and Salama 2021; R. S. Salama et al. 2020; R. S. Salama, El-Sayed, et al. 2021; R. S. Salama, Mannaa, et al. 2021; R. S. Salama, El-Bahy, and Mannaa 2021), due to the insertion of the second metal ions in the same frameworks. One of the representative examples is the fruitful synthesis of multivariate metal organic frameworks (MTV-MOFs), described by Omar Yaghi, in which up to eight different organic linkers were combined into one single framework (Deng et al. 2010).

The main object of the present work is to investigate the potential of mixed component metal organic frameworks (Cu_x-Cr_{100-x}–MOF) as an adsorbent material for removal of MO from aqueous solutions. The different parameters such as effect of the pH, adsorbent dosage, initial dye concentration and contact time that effects on the sorption process of methyl orange onto Cu_x-Cr_{100-x}–MOF were investigated. The isotherms and kinetics parameters for the adsorption of methyl orange onto Cu_x-Cr_{100-x}–MOF were calculated. Remarkably, Cu_{75}-Cr_{25}-MOF exhibits higher adsorption performance with maximum adsorption capacity equal 342.5 mg/g.

2. Material and methods

2.1. Materials

Copper (II) nitrate trihydrate ($Cu(NO_3)_2.3H_2O$, 98.5%) and Chromium trinitrate ($Cr(NO_3)_3.9H_2O$, 98.5%) were purchased from Sigma-Aldrich chemical reagent co., terephthalic acid or benzene 1, 4-dicarboxylic acid ($C_8H_6O_4$, 99+%) and methyl orange dye were purchased from Alfa Aesar. N, N-dimethylformamide ((DMF ≥ 99.5%), ethanol (≥ 99.5%) were commercially purchased from Alfa Aesar and used without further purification.

2.2 adsorbent preparation

Cu_x-Cr_{100-x}–MOF was synthesized through a hydrothermal method according to the reported approach with slightly modified procedure (Kozachuk et al. 2012). The mixed-metal MOFs were synthesized by changing the ratios of the chromium and copper precursors. The reaction mixtures with molar compositions of 0.10 $Cu(NO_3)_2{\cdot}3H_2O$ (48 mg)/0.90 $Cr(NO_3)_3{\cdot}6H_2O$ (622 mg)/ H_2bdc (332 mg) **(i),** 0.25 $Cu(NO_3)_2{\cdot}3H_2O$ (120 mg)/0.75 $Cr(NO_3)_3{\cdot}6H_2O$ (519 g)/ H_2bdc (332 mg) **(ii)**, 0.50 $Cu(NO_3)_2{\cdot}3H_2O$ (241 mg)/0.50 $Cr(NO_3)_3{\cdot}6H_2O$ (346 mg)/ H_2bdc (332 mg) **(iii)**, 0.75 $Cu(NO_3)_2{\cdot}3H_2O$ (361 mg)/0.25 $Cr(NO_3)_3{\cdot}6H_2O$ (173 mg)/ H_2bdc (332 mg) **(iv)**, 0.90 $Cu(NO_3)_2{\cdot}3H_2O$ (434 mg)/0.10 $Cr(NO_3)_3{\cdot}6H_2O$ (69.2 mg)/ H_2bdc (332 mg) **(v)** were dissolved in 30 ml DMF and 10 ml deionized water for each synthesis. Then the mixtures were moved into a Teflon lined stainless steel autoclave then heated at 120 ^oC and preserved at that temperature for 48 h. After cooling, greenish Blue (according to the amount of chromium and copper) crystals were collected, washed one time with dimethyl formamide. Then for elimination of unreacted terephthalic acid stuck inside the pores, the product was washed with hot ethanol (70 ^oC) for 4 h, then filtered and dried at 60 ^oC for 12h.

2.3. Batch Adsorption Experiments

Batch adsorption experiments of methyl orange were carried out in a 50 mL stoppered bottle at a constant temperature (25 ± 0.2°C) using a shaking thermostat machine. The effect of pH on the adsorption of MO was examined by mixing 50 mg of Cu_{50}-Cr_{50}–MOF with 50 mL of methyl orange (100 ppm) solution with the pH ranging from 2.0 to 12.0. The pH of the samples was adjusted by adding micro liter quantities of 1 mol/L HCl or 1 mol/L NaOH. In kinetics studies, 50 mg of Cu_x-Cr_{100-x}–MOF was mixed with 50 mL of MO solution with initial concentrations 200 ppm, and samples were withdrawn at desired time intervals. In isotherm experiments, 50 mg of Cu_x-Cr_{100-x}–MOF was added to 50 mL of MO solution with varied initial concentrations (50–500 ppm).

After adsorption, the samples were centrifuged using a centrifuge machine at a speed of 4000 r/min. The concentrations of methyl orange in aqueous solution were determined by using standard curve. The absorbance of MO in aqueous solutions was measured with a Shimadzu UV-1601PC spectrophotometer at 465 nm. Before each measurement, the base line of spectrophotometer was calibrated against solvent. The standard curve was obtained by plotting absorbance versus concentration of MO.
The amount of MO adsorbed (q_e) was determined by using the following equation:

$$q_e = \frac{[(C_0 - C_e)V]}{W} \qquad (1)$$

Where, C_e and C_o are equilibrium and initial concentrations of MO (mg/L), respectively, w (g) is the samples weight and V (L) is the volume of MO solution (50 ml).

3. Results and discussions

3.1. adsorption studies: -

3.1.1 The effect of pH:

One of the most vital parameters for whole adsorption process is pH adjusting of dye solution that influencing not only the active sites charge of adsorbent but also the ionization degree of MO solution during the adsorption process (Song et al. 2016). Therefore, in this work, pH was studied in the range of 2.0 – 12.0 using initial dye concentration of 100 ppm as shown in Fig. 1. This figure shows that the adsorbed amount of MO at equilibrium (q_e) decreases from 93.4 to 14.5 mg/g as the pH changes from 2 to 12. The decrease in concentration of the dyes adsorbed at different pH may be due to different reasons. It could be as a result of the degree of ionization of the species at the different pH. More methyl orange was absorbed by Cu_{50}-Cr_{50}–MOF powder in an acid medium. So, the pH of the medium affects the quantity of the adsorbent adsorbed by a given adsorbent and from these results, the optimum pH was frequently reported to be at about pH 2.0.

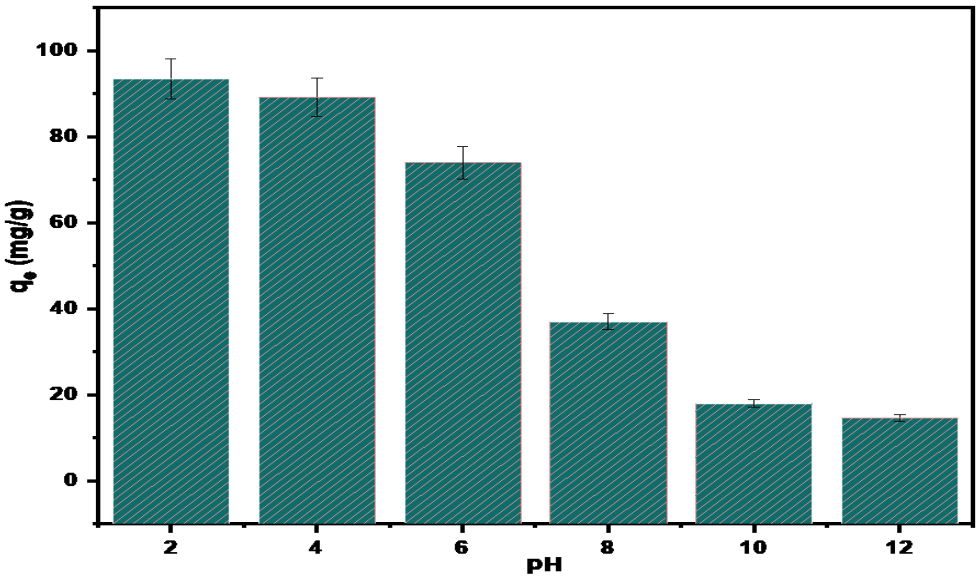

Fig. 1: Effect of initial pH on the adsorption of MO on Cu_{50}-Cr_{50}–MOF (adsorbent dosage = 50 mg, initial MO concentration = 100 ppm, solution volume = 50ml, temperature = 25°C, contact time = 90min).

3.1.2. Effect of initial dye concentration and adsorption isotherms:

Pure Cu-BDC, Cr-MIL-101 and mixed Cu_x-Cr_{100-x}–MOF materials are very active for the methyl orange adsorption from aqueous solution. The adsorption capacities of methyl orange under these experimental conditions are summarized in table 1. The combination between copper and chromium in the same framework showed a better adsorption capacity compared to pure Cu-BDC and Cr-MIL-101as shown in table 1.

The removal percentage of methyl orange at different initial concentrations were investigated as shown in Fig. 2. The removal percentage of MO reduced progressively when the concentration of MO increases from 50 ppm to 500 ppm. At a moderately low concentration (50 ppm), all adsorbents can totally remove methyl orange from aqueous solution. At a higher concentration of dye (250 ppm), Cu_{50}-Cr_{50}–MOF and Cu_{75}-Cr_{25}–MOF can still

cause complete removal of dye. Evidently, both Cu_{50}-Cr_{50}–MOF and Cu_{75}-Cr_{25}–MOF material show higher adsorption ability for MO removal than other adsorbents.

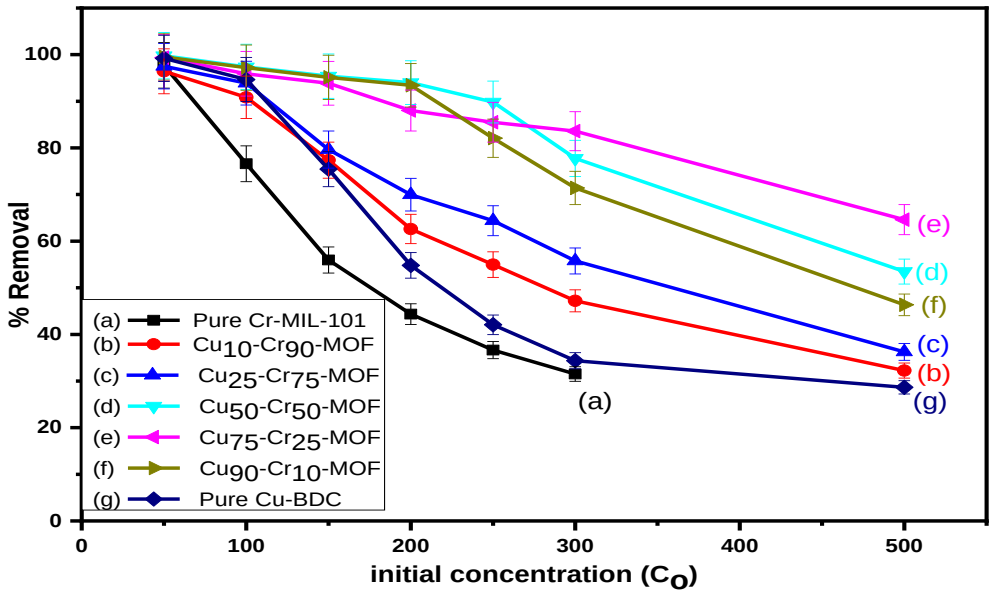

Fig. 2: Effect of MO concentration on the adsorption performance over Mixed MOFs.

Table 1 showed that the adsorption capacity Cu_x-Cr_{100-x}–MOF was increased with increase the copper content which may be due to the synergetic effect of Cu (II) and Cr (III) on methyl orange (MO) molecule, which enhanced the ability of methyl orange adsorption on mixed MOFs (Song et al. 2016). While, if more copper were introduced into the framework, it may block the pore and lead to the increase of diffusion reactions, which can actually decrease the amount of accessible active sites (Song et al. 2016), and thus, the Cu_{90}-Cr_{10}–MOF shows a smaller MO uptake capacity than that with lower Cu (II) in the framework. Therefore, among all the samples, Cu_{75}-Cr_{25}–MOF shows the highest methyl orange dye capacity.

The analysis and design of the adsorption process requires the relevant adsorption equilibrium, which is the most important piece of information in understanding an adsorption process. Fig. 3 shows Langmuir adsorption isotherm.

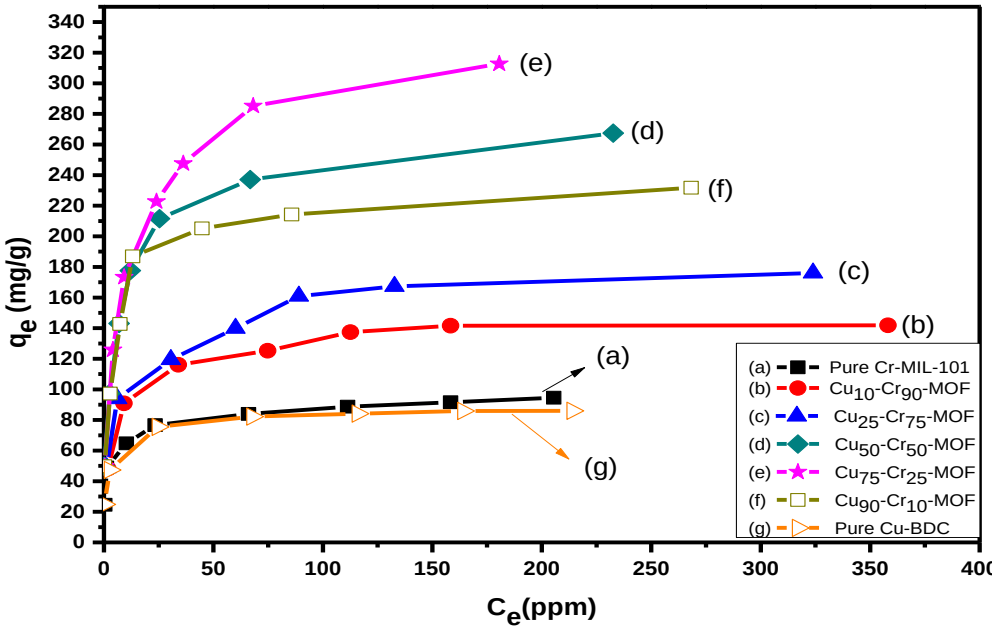

Fig. 3: Equilibrium adsorption isotherm of Methyl orange over Mixed MOFs.

The adsorption behavior of MO on pure Cu-BDC, Cr-MIL-101 and Cu_x-Cr_{100-x}–MOF can be further study. Based on the adsorption equilibrium data, there are two adsorption isotherm equations of Langmuir and Freundlich isotherm models were applied. **Firstly**, The Langmuir isotherm is given by Equation (2).

$$\frac{C_e}{q_e} = \frac{1}{q_m k_L} + \frac{C_e}{q_m} \qquad (2)$$

Maximum adsorption capacity q_m and Langmuir constants k_L values are listed in Table 1 which are calculated from the isotherms shown in Fig. 4. The main features of Langmuir adsorption isotherm can be expressed in terms of equilibrium parameter or separation factor (R_L), which defined by equation (3).

$$R_L = \frac{1}{(1 + k_L C_o)} \qquad (3)$$

From Table 1, all magnitudes of R_L are exist between 0 and 1 which demonstrates that methyl orange adsorption over Pure Cu-BDC, Cr-MIL-101 and Cu_x-Cr_{100-x}–MOF samples from water is favorable.

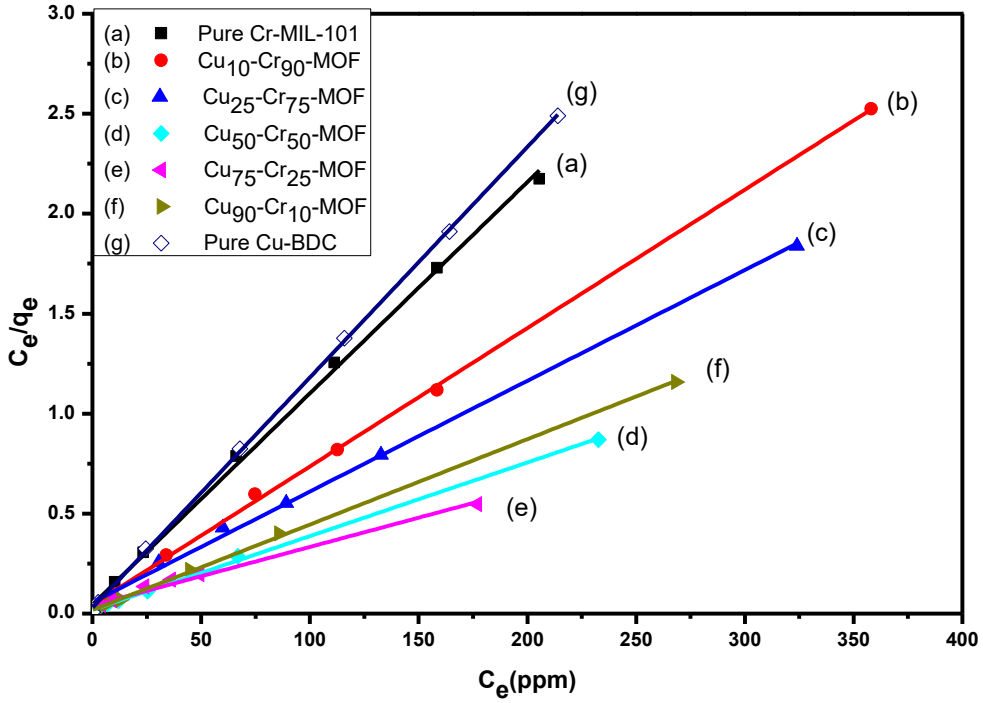

Fig. 4: Linear form of Langmuir isotherm of methyl orange over Mixed MOFs.

Secondly, the surface heterogeneity was examined by Freundlich model which is given by Equation (4)

$$Log\ q_e = \frac{1}{n}\ Log\ C_e + Log\ K_F \qquad (4)$$

The parameter n and k_F are calculated from fitted isotherm that shown in Fig. 5. The estimated values of k_F and 1/n were represented in table 1. The slope (1/n) value used to determine the surface heterogeneity which ranged from zero to one and heterogeneity is high if the slope value closer to zero (Hu, Deibert, and Li 2014). The values of k_F and 1/n obtained in this study shows that methyl orange adsorption over Pure Cu-BDC, Cr-MIL-101 and Cu_x-Cr_{100-x}–MOF samples favored by positive cooperatively binding and heterogeneous in nature.

From table 1, it was evident that the Langmuir model was clearly the most suitable to describe the adsorption process due to its high correlation coefficients (R^2) compared to the data obtained from Freundlich model.

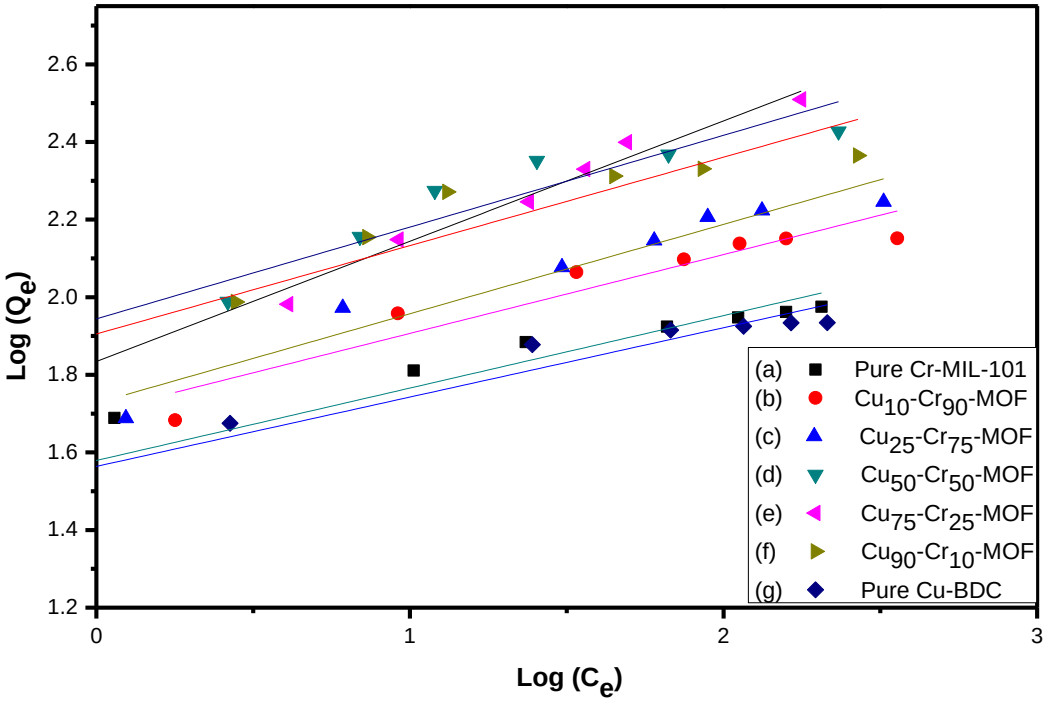

Fig. 5: Linear form of Freundlich isotherm of methyl orange over mixed MOFs.

3.1.3 Dynamic adsorption of methyl orange:

One of the most important techniques used to evaluate the adsorption performance is kinetic study which describes the rate of adsorbate uptake above pure Cu-BDC, Cr-MIL-101 and Cu_x-Cr_{100-x}–MOF samples and the equilibrium time. The amount of dye adsorbed at time t, q_t (mg/g) was calculated using equation (5).

$$q_e = \frac{[(C_0 - C_t)V]}{W} \qquad (5)$$

Where, C_o is initial concentrations of MO (mg/L), C_t is concentrations of MO at any time (mg/L), w (g) is the samples weight and V (L) is the volume of MO solution (50 ml).

Fig. 6 shows the evolution of the amount of adsorbed MO at any time (q_t) with contact time (t) over pure Cu-BDC, Cr-MIL-101 and Cu_x-Cr_{100-x}–MOF using initial dye concentration (C_o=200 ppm) at pH = 2. The figure shows that adsorption of methyl orange was extremely fast in the first 30 min, then progressively decreases within increases contact time until reaches 90 min. Equilibrium was attained after 90 min and there is no extra growth in adsorption capacity with more increase in contact time. From these results, the equilibrium time in the adsorption experiments was taken as 90 min.

Numerous steps were used to observe the adsorption kinetics controlling of sorption process like diffusion control, mass transfer and chemical reaction. Pseudo 1st order and pseudo 2nd order models used for MO adsorption over pure Cu-BDC, Cr-MIL-101 and Cu_x-Cr_{100-x}–MOF. The similarity between the predicted values and experimental data was expressed by the correlation coefficients R^2 (Li, Kuppler, and Zhou 2009).

The formula of pseudo 1st order kinetic model is given by equation (6):

$$Log\ (q_e - q_t) = Log(q_e) - \left(\frac{k_1}{2.303}\right)t \qquad (6)$$

Where q_t (mg/g) act as adsorption capacity of MO at any time (t) and q_e (mg/g) is the adsorption capacity at equilibrium time, and k_1 (min^{-1}) is the rate constant of pseudo 1st order adsorption.

On the other hand, pseudo 2nd order kinetic model is expressed by the equation (7):

$$\frac{t}{q_t} = \frac{1}{k_2 q_e^2} + \frac{t}{q_e} \qquad (7)$$

Where K_2 (g/ (mg. min^{-1})) is the rate constant of pseudo 2nd order adsorption that could be calculated from linear plot of t/q_t against time.

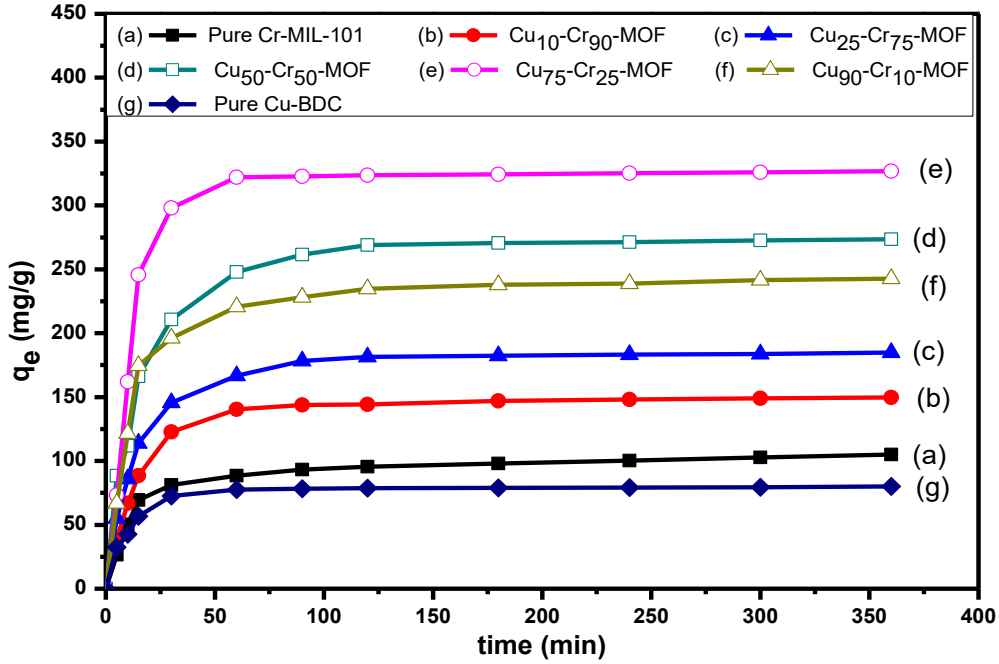

Fig. 6: Kinetic adsorption curves of methyl orange using initial dye concentration (C_o = 200 ppm) over mixed MOFs.

Fig. 7 and Fig. 8 show the application of linear pseudo first and second order model to the kinetic adsorption. The evaluated kinetic parameters and correlation coefficient (R^2) from kinetic models are summarized in table 2. The variance between calculated q_m and theoretical q_e and low R^2 value indicate that the pseudo 1st order wasn't well matched to describe the adsorption of methyl orange over pure Cu-BDC, Cr-MIL-101 and Cu_x-Cr_{100-x}–MOF. From another point of view, pseudo 2nd order model was considered as the best-fit model in description of methyl orange adsorption from aqueous solution. It's clear that the rate of adsorption of MO was controlled largely by chemical process which mostly involved ion exchange.

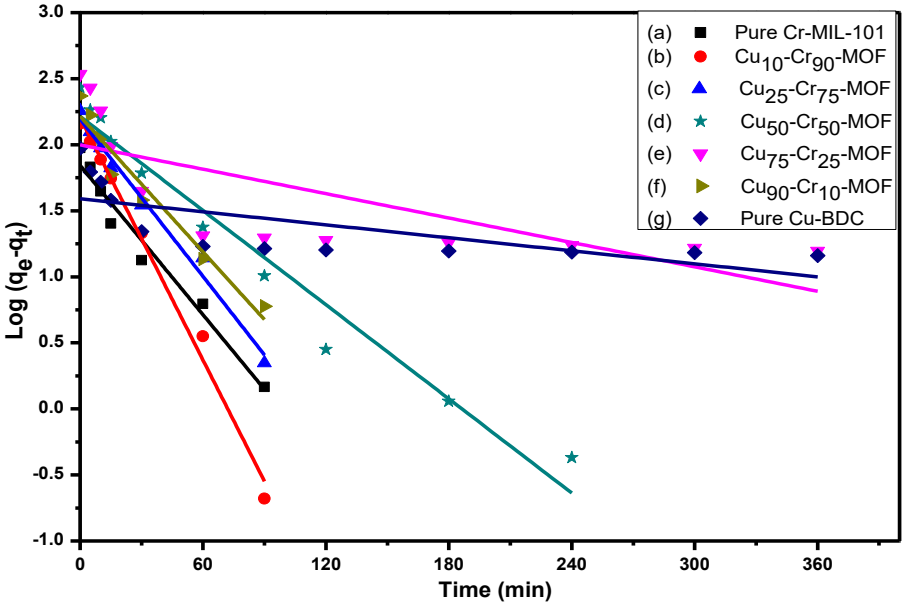

Fig. 7: Pseudo 1st order kinetic model for adsorption of MO above mixed MOFs.

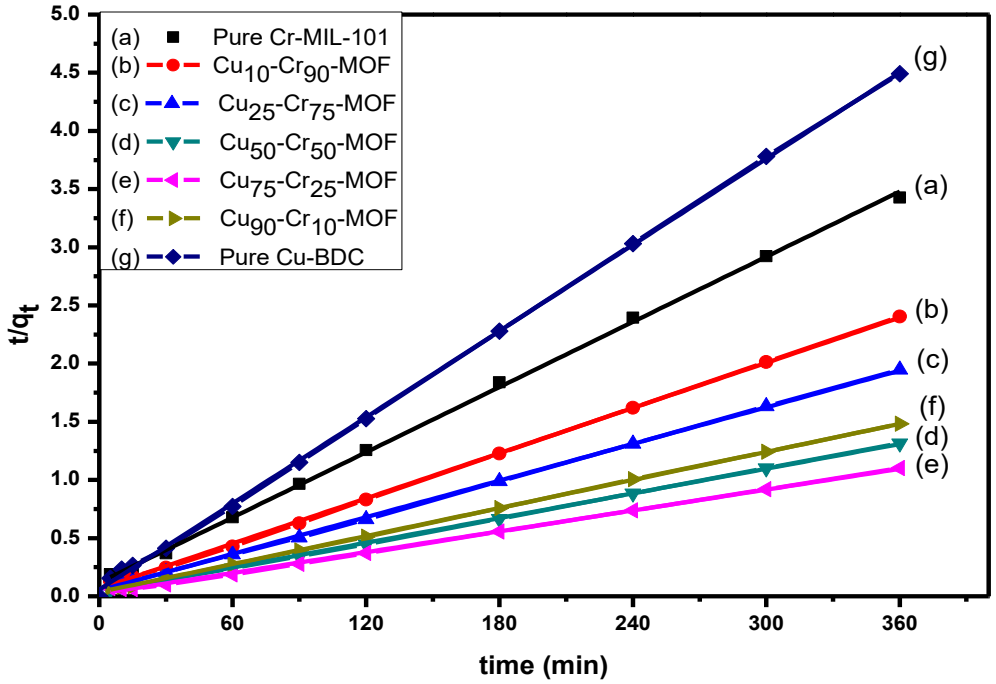

Fig. 8: Pseudo 2nd order kinetic model for adsorption of MO above mixed MOFs.

3.1.4 Adsorption mechanism

To predict the rate limiting step both intraparticle diffusion and Boyd plots are applied. From intraparticle diffusion plot as in Fig. 9, it is shown that the lines don't pass through the origin, therefore Intraparticle diffusion is not the only rate limiting step and indicates the effect of film diffusion (boundary layer diffusion). From Boyd plot, Fig. 10, it was observed that the plots are linear but do not pass though the origin suggesting that the adsorption process is controlled by film diffusion for all samples. Intra-particle diffusion and Boyd plot parameters for adsorption of methyl orange onto investigated adsorbent are shown in table 3.

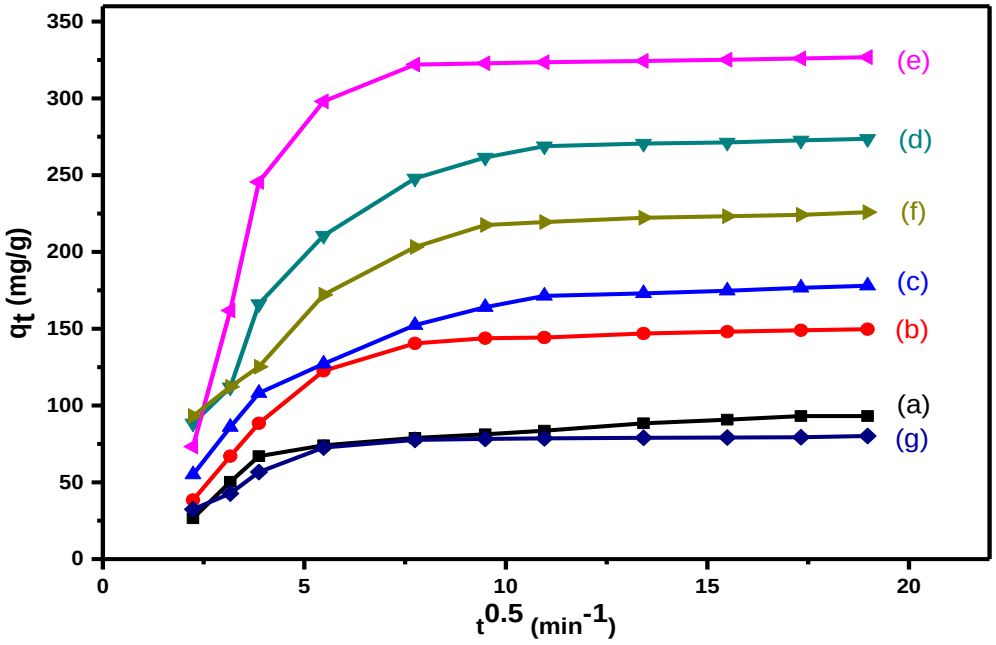

Fig. 9: Intraparticle diffusion plot for adsorption of methyl orange onto (a) Pure Cr-MIL-101; (b) Cu_{10}-Cr_{90}–MOF, (c) Cu_{25}-Cr_{75}–MOF, (d) Cu_{50}-Cr_{50}–MOF, (e) Cu_{75}-Cr_{25}–MOF, (f) Cu_{90}-Cr_{10}–MOF and (g) Cu-BDC.

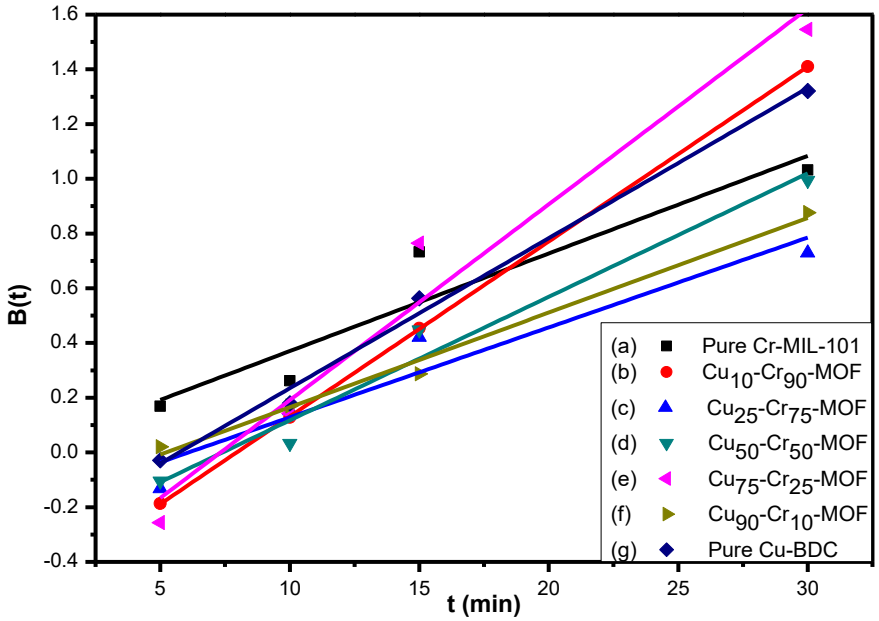

Fig. 10: Boyd plots for adsorption of methyl orange onto mixed MOFs.

Table 1: Estimated constants of Langmuir and Freundlich isotherms for MO adsorption over mixed MOFs.

Sample name	Langmuir isotherm				Freundlich isotherm		
	q_m (mg/g)	k_L (L/mg)	R_L	R^2	k_F	1/n	R^2
Pure Cr-MIL-101	94.6	0.2362	0.0139	0.9982	37.948	0.1867	0.8708
Cu_{10}-Cr_{90}–MOF	144.5	0.1572	0.0126	0.9994	50.541	0.2031	0.8841
Cu_{25}-Cr_{75}–MOF	180.5	0.0978	0.0201	0.9976	53.345	0.2303	0.9356
Cu_{50}-Cr_{50}–MOF	271.7	0.0915	0.0214	0.9983	68.278	0.2365	0.9381
Cu_{75}-Cr_{25}–MOF	342.5	0.0713	0.0273	0.9834	87.927	0.3099	0.9876
Cu_{90}-Cr_{10}–MOF	234.2	0.2339	0.0085	0.9993	80.397	0.2277	0.8972
Pure Cu-BDC	86.71	0.40306	0.0473	0.9997	36.643	0.1786	0.9477

Table 2: kinetics parameters for adsorption of methyl orange (200 mg/L) over mixed MOFs.

Sample name	Experimental q_m (mg/g)	Pseudo 1st order kinetics			Pseudo 2nd order kinetics		
		q_e (mg/g)	k_1 (min^{-1})	R^2	q_e (mg/g)	k_2 (g/(mg.min))	R^2
Pure Cr-MIL-101	94.6	44.1	0.0105	0.9151	95.7	0.00064	0.9991
Cu_{10}-Cr_{90}–MOF	144.5	160.79	0.0705	0.9896	149.2	0.00069	0.9995
Cu_{25}-Cr_{75}–MOF	180.5	155.97	0.0457	0.9838	182.4	0.000601	0.9997
Cu_{50}-Cr_{50}–MOF	271.7	163.82	0.0274	0.9623	274.1	0.000375	0.9996
Cu_{75}-Cr_{25}–MOF	342.5	99.76	0.0071	0.5015	339.3	0.000402	0.9986
Cu_{90}-Cr_{10}–MOF	234.2	163.80	0.0394	0.9444	238.7	0.000486	0.9997
Pure Cu-BDC	86.71	38.94	0.0037	0.4556	80.97	0.000266	0.9995

Table 3: Intra-particle diffusion and Boyd plot parameters for adsorption of MO over mixed MOFs:

Samples	Intraparticle diffusion			Boyd plot	
	k_d (mg/g.h$^{0.5}$)	C (mg/gm)	R^2	Intercept	R^2
Pure Cr-MIL-101	14.26	1.88	0.7813	0.0136	0.8511
Cu_{10}-Cr_{90}–MOF	25.80	7.04	0.9843	0.0639	0.9998
Cu_{25}-Cr_{75}–MOF	28.82	13.63	0.8953	0.0328	0.8912
Cu_{50}-Cr_{50}–MOF	39.31	25.41	0.9392	0.0451	0.9617
Cu_{75}-Cr_{25}–MOF	69.04	41.32	0.8804	0.0715	0.9489
Cu_{90}-Cr_{10}–MOF	24.43	35.56	0.9819	0.0346	0.9864
Pure Cu-BDC	12.65	4.47	0.9752	0.0549	0.9912

4. Conclusion

Copper and chromium bi-metallic organic frameworks (MOFs) were synthesized by reaction of 1, 4 benzene dicarboxylic acid as a linker with chromium nitrate and copper nitrate at different mole ratios as metal ion sources. The adsorption isotherms and kinetics study of methyl orange removal from water were investigated spectrophotometrically using the batch adsorption technique. The effect of initial dye concentration, adsorbent dosage and pH of the medium were investigated. The adsorption rate and the capacity were found to increase as adsorbent dosage increased but decreases as initial concentration of methyl orange increases, this may be due to the fact that the active sites of adsorbent can adsorb a certain concentration of dye. It was also found that the pH of the solution determines the concentration of dye that would be adsorbed on to mixed MOFs. The adsorption isotherms and adsorption kinetics also were studied and the data obtained fits well onto Langmuir isotherm and pseudo 2nd order kinetics, respectively. Mixed component metal organic frameworks (Cu_x-Cr_{100-x}–MOF) are a promising adsorbent which can used to clean up textile wastes.

Disclosure

This research did not receive any specific grant from funding agencies in the public, commercial or not-for-profit sectors. There is no Conflict of Interest

References

Alshorifi, Fares T et al. 2021. “Facile and Green Synthesis of Silver Quantum Dots Immobilized onto a Polymeric CTS–PEO Blend for the Photocatalytic Degradation of p-Nitrophenol.” *ACS Omega* 6: 30432–41.

Altass, Hatem M, Moataz Morad, et al. 2021. “Enhanced Catalytic Activity for CO Oxidation by Highly Active Pd Nanoparticles Supported on Reduced Graphene Oxide/Copper Metal Organic Framework.” *Journal of the Taiwan Institute of Chemical Engineers* 128: 194–208.

Altass, Hatem M, Abdelrahman S Khder, et al. 2021. “Highly Efficient, Recyclable Cerium-Phosphate Solid Acid Catalysts for the Synthesis of Tetrahydrocarbazole Derivatives by Borsche–Drechsel Cyclization.” *Reaction Kinetics, Mechanisms and Catalysis* 134: 143–61.

Altass, Hatem M et al. 2022. “Exploitation the Unique Acidity of Novel Cerium-Tungstate Catalysts in the Preparation of Indole Derivatives under Eco-Friendly Acid Catalyzed Fischer Indole Reaction Protocol.” *Arabian Journal of Chemistry* 15(3): 103670.

Alzaydien, Atef S. 2015. “Adsorption Behavior of Methyl Orange onto Wheat Bran: Role of Surface and PH.” *Oriental journal of chemistry* 31(2): 643.

Bakry, Ayyob M et al. 2022. “Remediation of Water Containing Phosphate Using Ceria Nanoparticles Decorated Partially Reduced Graphene Oxide (CeO2-PRGO) Composite.” *Surfaces and Interfaces* 31: 102006.

Chen, Chen, Meng Zhang, Qingxin Guan, and Wei Li. 2012. “Kinetic and Thermodynamic Studies on the Adsorption of Xylenol Orange onto MIL-101 (Cr).” *Chemical Engineering Journal* 183: 60–67.

Crini, Gregorio. 2006. “Non-Conventional Low-Cost Adsorbents for Dye Removal: A Review.” *Bioresource technology* 97(9): 1061–85.

Deng, Hexiang et al. 2010. "Multiple Functional Groups of Varying Ratios in Metal-Organic Frameworks." *Science* 327(5967): 846–50.

Eddaoudi, Mohamed et al. 2001. "Modular Chemistry: Secondary Building Units as a Basis for the Design of Highly Porous and Robust Metal− Organic Carboxylate Frameworks." *Accounts of chemical research* 34(4): 319–30.

El-Dafrawy, Shady M, Reda S Salama, Sohier A El-Hakam, and Salem E Samra. 2020. "Bimetal-Organic Frameworks (Cux-Cr100-x–MOF) as a Stable and Efficient Catalyst for Synthesis of 3, 4-Dihydropyrimidin-2-One and 14-Phenyl-14H-Dibenzo [a, j] Xanthene." *Journal of Materials Research and Technology* 9(2): 1998–2008.

El-Hakam, S. A. et al. 2021. "Greener Route for the Removal of Toxic Heavy Metals and Synthesis of 14-Aryl-14H Dibenzo[a,j] Xanthene Using a Novel and Efficient Ag-Mg Bimetallic MOF as a Recyclable Heterogeneous Nanocatalyst." *Journal of the Taiwan Institute of Chemical Engineers* 122: 176–89. https://doi.org/10.1016/j.jtice.2021.04.036.

El-Hakam, S.A. et al. 2018. "Synthesis of Sulfamic Acid Supported on Cr-MIL-101 as a Heterogeneous Acid Catalyst and Efficient Adsorbent for Methyl Orange Dye." *RSC Advances* 8(37): 20517–33.

El-Hakam, S A et al. 2013. "Surface Acidity and Catalytic Activity of Sulfated Titania Supported on Mesoporous MCM-41." *Int. J. Modern Chem* 5(1): 55–70.

El-Hakam, Sohier A. et al. 2018. "Synthesis of Sulfamic Acid Supported on Cr-MIL-101 as a Heterogeneous Acid Catalyst and Efficient Adsorbent for Methyl Orange Dye." *RSC Advances* 8(37): 20517–33.

El-Hakam, Sohier A et al. 2022. "Application of Nanostructured Mesoporous Silica/Bismuth Vanadate Composite Catalysts for the Degradation of Methylene Blue and Brilliant Green." *Journal of Materials Research and Technology* 18: 1963–76.

El-Yazeed, Wafaa S Abo et al. 2022. "Ag-PMA Supported on MCM-41: Surface Acidity and Catalytic Activity." *Journal of Sol-Gel Science and Technology* 102: 387–399.

Horcajada, Patricia et al. 2011. "Metal–Organic Frameworks in Biomedicine." *Chemical reviews* 112(2): 1232–68.

Hu, Zhichao, Benjamin J Deibert, and Jing Li. 2014. "Luminescent Metal–Organic Frameworks for Chemical Sensing and Explosive Detection." *Chemical Society Reviews* 43(16): 5815–40.

Ibrahim, Amr A et al. 2021. "Synthesis of 12-Tungestophosphoric Acid Supported on Zr / MCM-41 Composite with Excellent Heterogeneous Catalyst and Promising Adsorbent of Methylene Blue." *Colloids and Surfaces A : Physicochemical and Engineering Aspects* 631(August): 127753.

Kozachuk, Olesia et al. 2012. "Microporous Mixed-Metal Layer-Pillared [Zn1–XCux (Bdc)(Dabco) 0.5] MOFs: Preparation and Characterization." *European Journal of Inorganic Chemistry* 2012(10): 1688–95.

Li, Jian-Rong, Ryan J Kuppler, and Hong-Cai Zhou. 2009. "Selective Gas Adsorption and Separation in Metal–Organic Frameworks." *Chemical Society Reviews* 38(5): 1477–1504.

Li, Jian-Rong, Julian Sculley, and Hong-Cai Zhou. 2011. "Metal–Organic Frameworks for Separations." *Chemical reviews* 112(2): 869–932.

Ma, Jie et al. 2012. "Enhanced Adsorptive Removal of Methyl Orange and Methylene Blue from Aqueous Solution by Alkali-Activated Multiwalled Carbon Nanotubes." *ACS applied materials & interfaces* 4(11): 5749–60.

Mannaa, Mohammed A et al. 2021. "Role of NiO Nanoparticles in Enhancing Structure Properties of TiO2 and Its Applications in Photodegradation and Hydrogen Evolution." *ACS omega* 6(45): 30386–400.

Mannaa, Mohammed A, Hatem M Altass, and Reda S Salama. 2021. "MCM-41 Grafted with Citric Acid: The Role of Carboxylic Groups in Enhancing the Synthesis of Xanthenes and Removal of Heavy Metal Ions." *Environmental Nanotechnology, Monitoring & Management* 15: 100410.

Nigam, P. 2007. "Color Removal from Textile Waste Water Using Bioculture in Continuous Mode." *Biores Technol* 77: 247–55.

Puvaneswari, N, J Muthukrishnan, and P Gunasekaran. 2006. "Toxicity Assessment and Microbial Degradation of Azo Dyes."

Radha, K V, I Regupathi, A Arunagiri, and T Murugesan. 2005. "Decolorization Studies of Synthetic Dyes Using Phanerochaete Chrysosporium and Their Kinetics." *Process Biochemistry* 40(10): 3337–45.

Ranocchiari, Marco, and Jeroen Anton van Bokhoven. 2011. "Catalysis by Metal–Organic Frameworks: Fundamentals and Opportunities." *Physical Chemistry Chemical Physics* 13(14): 6388–96.

Reda S. Salama Salem. E. Samra, Shady M. El-Dafrawy and Awad I. Ahmed, Sohier A El-Hakam. 2018. "Cu-BDC as a Novel and Efficient Catalyst for the Synthesis of 3,4-Dihydropyrimidin-2(1H)-Ones and Aryl-14H-Dibenzo [a, j] Xanthenes under Conventional Heating." *International Journal of Nano and Material Sciences* 7(1): 31–42.

Sahiner, Nurettin, Sahin Demirci, and Mustafa Yildiz. 2017. "Preparation and Characterization of Bi-Metallic and Tri-Metallic Metal Organic Frameworks Based on Trimesic Acid and Co (II), Ni (II), and Cu (II) Ions." *Journal of Electronic Materials* 46(2): 790–801.

Salama, Reda et al. 2022. "Synthesis, Characterization of Titania Supported on Mesoporous MCM-41 and Its Application for the Removal of Methylene Blue." *Delta University Scientific Journal* 5(2): 321–39.

Salama, Reda S., Mohammed A. Mannaa, et al. 2021. "Palladium Supported on Mixed-Metal-Organic Framework (Co-Mn-MOF-74) for Efficient Catalytic Oxidation of CO." *RSC Advances* 11(8): 4318–26.

Salama, Reda S., Salah M. El-Bahy, and Mohammed A. Mannaa. 2021. "Sulfamic Acid Supported on Mesoporous MCM-41 as a Novel, Efficient and Reusable Heterogenous Solid Acid Catalyst for Synthesis of Xanthene, Dihydropyrimidinone and Coumarin Derivatives." *Colloids and Surfaces A: Physicochemical and Engineering Aspects* 628(June): 127261.

Salama, Reda S., El Sayed M. El-Sayed, Salah M. El-Bahy, and Fathi S. Awad. 2021. "Silver Nanoparticles Supported on UiO-66 (Zr): As an Efficient and Recyclable Heterogeneous Catalyst and Efficient Adsorbent for Removal of Indigo Carmine." *Colloids and Surfaces A: Physicochemical and Engineering Aspects* 626(May): 127089.

Salama, Reda S et al. 2018a. "Adsorption, Equilibrium and Kinetic Studies on the Removal of Methyl Orange Dye from Aqueous Solution by Using of Copper Metal Organic Framework (Cu-BDC)." *Int. J. Modern Chem* 10(2): 195–207.

Salama, Reda S et al. 2018b. "Adsorption, Equilibrium and Kinetic Studies on the Removal of Methyl Orange Dye from Aqueous Solution by Using of Copper Metal Organic Framework (Cu-BDC)." *Int. J. Modern Chem* 10(2): 195–207.

Salama, Reda S et al. 2018c. "Cu-BDC as a Novel and Efficient Catalyst for the Synthesis of 3, 4-Dihydropyrimidin-2 (1H)-Ones and Aryl-14H-Dibenzo [a, j] Xanthenes under Conventional Heating." *Int. J. Nano & Matl. Sci* 7(1): 31–42.

Salama, Reda S et al. 2019. "Synthesis, Characterization and Catalytic Activities of Sulfuric Acid Loaded on Copper Metal Organic Frameworks (Cu-BDC)." *Delta University Scientific Journal* 2(1): 2.

Salama, Reda S et al. 2020. "The Role of PMA in Enhancing the Surface Acidity and Catalytic Activity of a Bimetallic Cr–Mg-MOF and Its Applications for Synthesis of Coumarin and Dihydropyrimidinone Derivatives." *RSC Advances* 10(36): 21115–28.

Shady, M, Reda S Salama, Sohier A El-Hakam, and Salem E Samra. 2019. "Bimetal-Organic Frameworks (Cux-Cr100-x–MOF) as a Stable and Efficient Catalyst for Synthesis of 3, 4-Dihydropyrimidin-2-One and 14-Phenyl-14H-Dibenzo [a, j] Xanthene."

Song, Wen et al. 2016. "Adsorption–Desorption Behavior of Magnetic Amine/Fe3O4 Functionalized Biopolymer Resin towards Anionic Dyes from Wastewater." *Bioresource technology* 210: 123–30.

Suciu, Nicoleta A et al. 2012. "Pesticide Removal from Waste Spray-Tank Water by Organoclay Adsorption after Field Application: An Approach for a Formulation of Cyprodinil Containing Antifoaming/Defoaming Agents." *Environmental Science and Pollution Research* 19(4): 1229–36.

Sun, Zhiguo et al. 2015. "Ag–Cu–BTC Prepared by Postsynthetic Exchange as Effective Catalyst for Selective Oxidation of Toluene to Benzaldehyde." *Catalysis Communications* 59: 92–96.

Wang, Lisa J et al. 2014. "Synthesis and Characterization of Metal–Organic Framework-74 Containing 2, 4, 6, 8, and 10 Different Metals." *Inorganic chemistry* 53(12): 5881–83.

Zhang, Aiping, and Yan Fang. 2006. "Influence of Adsorption Orientation of Methyl Orange on Silver Colloids by Raman and Fluorescence Spectroscopy: PH Effect." *Chemical physics* 331(1): 55–60.